

## Gram-Charlier development of the atomic displacement factors into mineral structures: The case of samsonite, $\text{Ag}_4\text{MnSb}_2\text{S}_6$

LUCA BINDI<sup>1,\*</sup> AND MICHEL EVAIN<sup>2</sup>

<sup>1</sup>Dipartimento di Scienze della Terra, Università degli Studi di Firenze, Via La Pira, 4-I-50121 Firenze, Italy

<sup>2</sup>Laboratoire de Chimie des Solides, IMN, UMR C6502 CNRS, Université de Nantes, 2 rue de la Houssinière, BP32229, 44322 Nantes CEDEX 3, France

### ABSTRACT

During structure solution of Ag-, Cu-bearing minerals it is quite common to observe disorder.  $\text{Ag}^+$  and  $\text{Cu}^+$ , indeed, can occur in different, but overlapping sites. The typical way to deal with these kind of minerals in structure determination is to use a split-atom model. This approach, however, has several disadvantages and may give rise to ambiguities. A solution to the problem can be the use of higher order tensor elements in the expression of the structure factors (the “non-harmonic approach”). This alternative approach gives, in cases of highly overlapping electron densities, an equivalent description of the split-atom model.

The non-harmonic approach based upon a Gram-Charlier development of the atomic displacement factors can be useful in mineral sciences for the determination of still unknown structures. In addition, such an approach can be used to refine known structures with suspiciously high  $R$  values and/or high isotropic displacement parameters for the silver or copper atoms. As an example of the application of this method, we have reinvestigated the crystal structure of samsonite,  $\text{Ag}_4\text{MnSb}_2\text{S}_6$ .

**Keywords:** Crystal structure, samsonite, X-ray data, atomic displacement parameters

### INTRODUCTION

Several silver-bearing sulfosalts are known to occur in nature; however, for some of them, a full structural study remains to be accomplished. The lack of structural information can be related, on the one hand, to a lack of suitable crystals and, on the other hand, to the difficulty in describing the  $\text{Ag}^+$  or  $\text{Cu}^+$  electron density. If the former situation is easily understood, the latter one is more complex and should be related to the observation that both  $\text{Ag}^+$  or  $\text{Cu}^+$   $d^{10}$  elements easily adopt various complex asymmetric coordinations. It has been shown (Gaudin et al. 2001 and references therein) that those particular coordinations are due to an  $s/d$  orbital mixing and/or polarization factors. Therefore, it is quite common to observe, in space and time average,  $\text{Ag}^+$  or  $\text{Cu}^+$  in different, but overlapping sites. This certainly also favors the presence of strong ionic conductivity observed in some materials because the activation energy of the jumps from site to site is lowered by the easy density deformation. Whatever the situation, ion conducting or nonconducting, the structure appears as disordered.

One classical way to deal with disordered materials in structure determination is the use of a split-atom model. This approach has several disadvantages and may give rise to ambiguities. As demonstrated by Bachmann and Schultz (1984), the introduction in the refinement of additional positions with fractional site occupation factors does not necessarily mean that

those extra positions correspond to occupied equilibrium sites. This is certainly true in the case of fast ionic conductors, for which there exists a delocalization of an ionic species over a liquid-like structure. Apart from these physically nonmeaningful refined positions, the simultaneous refinement of overlapping atoms with partial occupancy usually gives rise to high correlations and unstable refinements, the closer the refined positions in a disordered structure, the higher the correlations and the less stable the refinement. A solution to that problem is the use of higher order tensor elements in the expression of the structure factors (the “non-harmonic approach”—Johnson and Levy 1974; Zucker and Schulz 1982). Indeed, initially used for true anharmonic atomic vibration, it has been shown to give an equivalent description, but with less parameters, than the split-atom model in cases of disorder with highly overlapping electron densities (Kuks 1992). This alternative approach, in particular the Gram-Charlier formalism which is recommended by the IUCr Commission on Crystallographic Nomenclature (Trueblood et al. 1996), provides an easier convergence of the refinement, due to much lower correlations between the refined parameters. One potential drawback of the method one should be aware of, however, consists in the possible negative regions one could find in the probability density functions (*pdf*), which then indicate the inadequacy of the results. In some situations, it may then be better to use only the Gaussian approximation, even though the resulting  $R$  factors may be higher. This problem being mastered, the non-harmonic approach has been successfully used over the past twenty years in solving numerous structures, both

\* E-mail: lbindi@geo.unifi.it

of nonconducting materials (van der Lee et al. 1993; Boucher et al. 1994; Gaudin et al. 1997) and of fast ion conducting phases (Kuhns and Heger 1979; Boucher et al. 1992, 1993; Evain et al. 1998). Recently it has been used in solving complex structures in the pearceite-polybasite mineral family (Evain et al. 2006a, 2006b; Bindi et al. 2006a, 2006b, 2006c).

In both the split-atom model and the non-harmonic approach, one should be aware that the refined coordinates do not have a simple physical meaning, because they are just the first order terms in the expansion of the conventional structure factor. Therefore, one must be very cautious in interpreting bond distances from such refinements. A proper way to interpret the refined parameters is by using the joint probability density function (*jpdf*), which can be directly calculated from the refined parameters. This function is the weighted superposition of the Fourier Transform of the atomic displacement factors of atoms of several sites. Meaningful distances can then be calculated from the modes (i.e., maxima) of *jpdf* maps. All these features, i.e., non-harmonic expansion, *jpdf* calculation, etc., are not included in every routine crystallographic package. A complete setup, including refinement, calculation of *pdf* and *jpdf* maps, plotting of potential curves, has been, however, incorporated in the Jana program suite for many years, in a very user-friendly way (Petricek and Dusek 2000).

The aim of the present paper is to show that the non-harmonic approach based upon a Gram-Charlier development of the atomic displacement factors can be useful in mineral sciences for the determination of still unknown structures. In addition, such an approach can be used to refine known structures with suspiciously high *R* values and/or high isotropic displacement parameters for the silver or copper atoms. As a case study, we have reinvestigated the crystal structure of samsonite,  $\text{Ag}_4\text{MnSb}_2\text{S}_6$ , previously determined by Edenharter and Nowacki (1974). Although their structural model is correct, Edenharter and Nowacki reported an *R* value of 7.3% [with a  $I > 2.33\sigma(I)$  level] and  $B_{\text{iso}}$  values of 3.40 and 4.89  $\text{\AA}^2$  for Ag1 and Ag2 sites, respectively (approximately three times the values observed for the other metals and for the sulfur atoms). To study the variation of the silver *pdf* intensity data were collected at room temperature, 100, and 400 K.

#### X-RAY CRYSTALLOGRAPHY AND CRYSTAL-STRUCTURE REFINEMENT

A crystal of samsonite was selected from a sample from St. Andreasberg in the Hartz (type-locality), belonging to the collection of the Museo di Storia Naturale, sezione di Mineralogia, Università di Firenze (catalog number 45016/G). A chemical analysis on the selected crystal by means of a JEOL-JXA 8600 electron microprobe confirmed the  $\text{Ag}_4\text{MnSb}_2\text{S}_6$  stoichiometry. The same crystal was then fixed at the tip of a glass capillary by means of solvent-free glue. The intensity measurements were carried out on a Bruker-Nonius Kappa CCD diffractometer, using graphite-monochromatized  $\text{MoK-L}_{2,3}$  radiation ( $\lambda = 0.71073 \text{ \AA}$ ). The high (400 K) and low (100 K) temperatures were achieved by means of an Oxford cryostream cooler. A rather high  $\sin(\theta)/\lambda$  cutoff ( $0.8 \text{ \AA}^{-1}$ ) was considered to enhance the atomic displacement parameter resolution. Intensity integration and standard Lorentz-polarization correction were performed with the Bruker-Nonius EvalCCD program package. Subsequent calculations were conducted with the Jana2006 program suite (Petricek et al. 2006), except for the crystal shape and dimension optimization, which were performed with X-shape (Stoe and Cie 1996), a code based on the Habitus program (Herrendorf 1993). Structure drawings were produced with the Diamond program (Brandenburg 2001). Absorption corrections performed with the Gaussian integration method were preferred to empirical or semi-empirical corrections to prevent any bias in the determination of the atomic displacement parameters.

With the room-temperature data set, the crystal structure was refined starting from the atomic coordinates given by Edenharter and Nowacki (1974). Convergence was quickly achieved to  $R = 0.0428$  for 2506 observed reflections [ $I > 2\sigma(I)$ ] and 0.0569 for all 3018 independent reflections and 60 parameters. At this stage, Fourier difference maps reveal important residuals (up to  $4.7 e/\text{\AA}^3$  in absolute value) mainly around Ag1 and Ag2 atoms (Figs. 1a and 2a). These residuals do not occur at random and exhibit typical refinement model inadequacy. A refinement of the crystal structure of samsonite by considering the non-ideal atomic sites (i.e., Ag1 and Ag2) as split-atom positions was attempted. Each Ag site was split into three sub-sites (taken from the  $\Delta F$ -Fourier map) with partial occupancy-factors and isotropic displacement parameters. The refinement failed because of the closeness of the positions, the strong overlapping of the electron densities that resulted and the high correlations ( $>0.999$ ) that it generated. The refinement assuming a split-atom model was therefore discarded and a refinement [starting again from the atomic coordinates given by Edenharter and Nowacki (1974)] using the “non-harmonic approach” was then considered. The introduction of third-order Gram-Charlier non-harmonic atomic displacement parameters for the two silver positions significantly improved the refinement to  $R = 0.0295$  for 81 parameters, with a drop of the residuals in the Fourier difference maps (maximum at  $1.78 e/\text{\AA}^3$ ). These residuals (Figs. 1b and 2b) are featureless around Ag1 and resemble, with much less

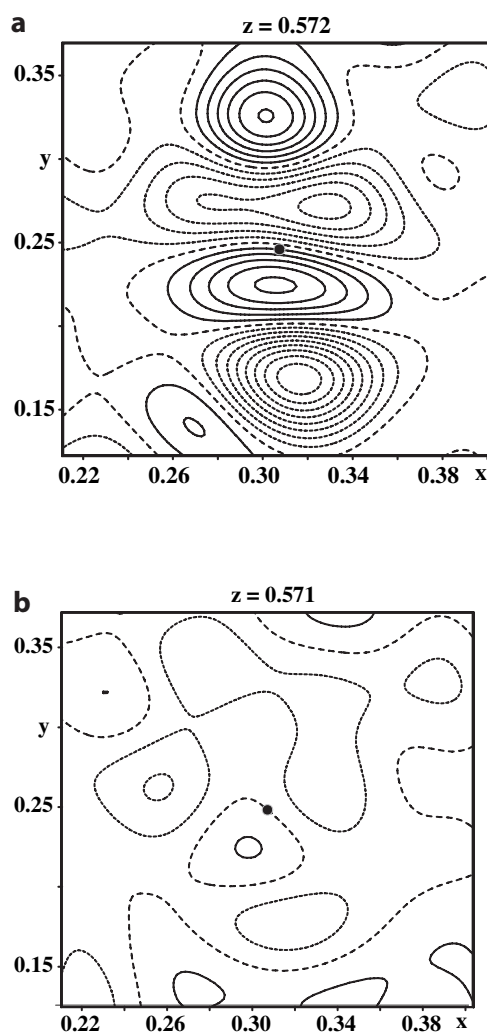


FIGURE 1. Difference Fourier maps for samsonite at RT, centered on Ag1 (label). Contour lines in intervals of  $0.5 e^{-3}$  for positive values (continuous lines) and negative values (dashed lines). (a) Second-order tensor (classical anisotropic parameters) and (b) third-order atomic displacement tensor for Ag1.

intensity, those previously seen around Ag2. The latter residuals around Ag2 can easily be removed with fourth order tensors, but with an unjustified increase of 15 parameters for a small  $R$  drop to 0.0271. Finally, with only third-order tensors for Ag1 and Ag2 and a secondary extinction coefficient, the refinement converged to the residual  $R$  value of 0.0282. The model is considered as valid since the negative part of the electron densities around Ag1 and Ag2 does not exceed, in absolute value, 1% of the probability density function maxima.

The model found for the room-temperature structure was taken as a starting point for the low-temperature (100 K) and high-temperature (400 K) structure refinements. It is worth noting that the Gram-Charlier development of the atomic displacement factors was not necessary at 100 K.  $R/wR$  values of 0.0352/0.0696 and 0.0553/0.0809 were obtained for the data sets collected at 100 and 400 K, respectively. The higher  $R$  values, as compared to the room temperature refinement, are due to less accurate data sets linked to the experimental setup (the use of the cryostream cooler).

Experimental details, final atomic coordinates, anisotropic displacement parameters, and higher-order parameters are reported in Tables 1–4, respectively.

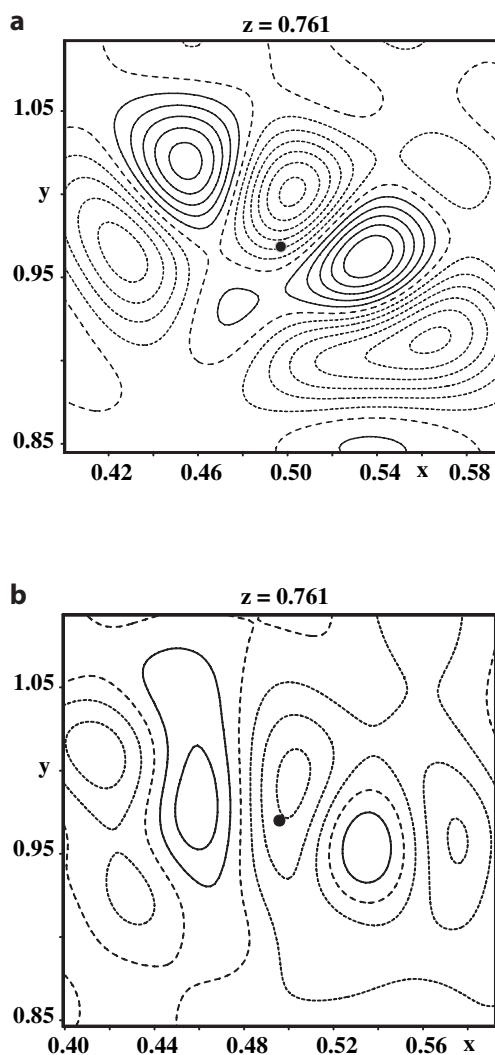


FIGURE 2. Difference Fourier maps for samsonite at RT, centered on Ag2 (label). Contour lines in intervals of  $0.5 e^{-} \times \text{Å}^{-3}$  for positive values (continuous lines) and negative values (dashed lines). (a) Second-order tensor (classical anisotropic parameters) and (b) third-order atomic displacement tensor for Ag2.

TABLE 1. Crystallographic data for samsonite

Temperature (K)	100	300	400
<b>Crystal data</b>			
Chemical formula	Ag <sub>4</sub> MnSb <sub>2</sub> S <sub>6</sub>		
Molecular weight (g/mol)	922.3		
Space group	P2 <sub>1</sub> /n		
Cell parameters:			
<i>a</i> (Å)	10.3702(8)	10.3861(6)	10.3838(9)
<i>b</i> (Å)	8.0647(7)	8.1108(7)	8.1364(8)
<i>c</i> (Å)	6.6400(7)	6.6630(7)	6.6737(7)
$\beta$ (°)	92.676(12)	92.639(12)	92.640(15)
<i>V</i> (Å <sup>3</sup> )	554.71(9)	560.69(8)	563.24(9)
<i>Z</i>	2		
Density, calc (g/cm <sup>3</sup> )	5.5199	5.4610	5.4363
Crystal color	black		
Crystal shape	block		
Crystal size (mm)	0.09 × 0.10 × 0.14		
<b>Data collection</b>			
Diffractometer	Bruker-Nonius KappaCCD		
Radiation	Mo <i>K</i> -L <sub>2,3</sub> (0.71073 Å)		
Monochromator	oriented graphite (002)		
Scan mode	$\phi/\omega$		
$\sin\theta/\lambda_{\text{max}}$ (Å <sup>-1</sup> )/ $\theta_{\text{max}}$ (°)	0.866/38.0		
Coverage (%) at $\theta_{\text{max}}$	98	99	98
<i>hkl</i> range	$-17 \leq h \leq 11$ $-10 \leq k \leq 13$ $-11 \leq l \leq 11$	$-17 \leq h \leq 17$ $-13 \leq k \leq 14$ $-11 \leq l \leq 11$	$-17 \leq h \leq 17$ $-13 \leq k \leq 14$ $-11 \leq l \leq 11$
No. of reflections	9297	18377	13597
<b>Data reduction</b>			
Linear abs. coeff. (mm <sup>-1</sup> )	13.878	13.730	13.668
Absorption correction	Gaussian integration method		
$T_{\text{min}}/T_{\text{max}}$	0.295/0.420	0.285/0.419	0.246/0.428
No. of independent refl.	2899	3018	3022
Criterion for obs.	$I > 2\sigma(I)$		
No. of observed refl.	2228	2506	1639
$R_{\text{int}}$	0.0516	0.0459	0.1027
<b>Refinement</b>			
Refinement coefficient	$F^2$		
F(000)	822		
No. of refl. in refinement	2899	3018	3022
No. of observed refl.	2228	2506	1639
No. of refined parameters	62	82	82
Weighting scheme	$w = 1/[\sigma^2(I) + (0.044 \times I)^2]$		
$R^w(\text{obs})/R^w(\text{all})$	0.0352 / 0.0614	0.0282 / 0.0416	0.0553 / 0.1464
$R^w(\text{obs})/R^w(\text{all})$	0.0696 / 0.0779	0.0742 / 0.0799	0.0809 / 0.1032
<i>S</i> (obs)/ <i>S</i> (all)	1.24 / 1.18	1.24 / 1.22	1.15 / 1.07
Secondary ext. coeff.†	0.060(9)	0.086(12)	0.043(11)
Diff. Fourier (e <sup>-</sup> /Å <sup>3</sup> )	[-2.83, 2.76]	[-1.26, 1.22]	[-2.49, 3.39]

\*  $R = \sum ||F_o| - |F_c|| / \sum |F_o|$ .  $R_w = [\sum w(|F_o|^2 - |F_c|^2)^2 / \sum w |F_o|^4]^{1/2}$ .

† Isotropic secondary extinction—Type I—Gaussian distribution (Becker and Coppens 1974).

## DESCRIPTION OF THE STRUCTURE

Apart from a much higher precision attained in the refinement, we found an atomic arrangement of samsonite at room temperature very similar to that reported by Edenharter and Nowacki (1974). In the samsonite structure (Fig. 3) the Mn atoms occupy slightly deformed MnS<sub>6</sub> octahedra and the Sb atoms are in a threefold coordination occupying the top of a trigonal pyramid with 3 S atoms forming the base. SbS<sub>3</sub> polyhedra are isolated from each other. The Ag atoms exhibit two different crystal-chemical environments: Ag1 is found to be tetrahedrally coordinated by four S atoms, whereas Ag2 is triangularly coordinated by three S atoms.

In Table 5, we report the bond distances in the structure of samsonite at the different temperatures. At room temperature the Sb-S bond distances (2.440–2.470 Å) match closely the value

observed commonly for covalent pure Sb-S bonds [2.47–2.48 Å in the structure of stephanite,  $\text{Ag}_5(\text{S})\text{SbS}_3$ , Ribár and Nowacki (1970); 2.418–2.422 Å in polybasite-221 and polybasite-222,  $(\text{Ag,Cu})_{16}(\text{Sb,As})_2\text{S}_{11}$ , respectively, Evain et al. (2006a); 2.452 Å in pyrrargirite  $\text{Ag}_3(\text{SbS}_3)$ , Engel and Nowacki (1966)].

The Ag1 position shows a regular tetrahedral environment with distances, calculated with the Ag1 mode position, ranging from 2.565 to 2.736 Å (Fig. 3). The average bond distance of 2.644 Å compares well with that found for the Ag(3) position in the crystal structure of stephanite (2.68 Å—Ribár and Nowacki 1970) and that found for the Ag(3) polyhedron in the

crystal structure of the synthetic  $\text{Ag}_7\text{S}_2[\text{AsS}_4]$  (2.642 Å—Pertlik 1994). Ag2 (Fig. 3) is triangularly coordinated by S atoms, showing two shorter bond distances with the S1 and S2 atoms (2.397 and 2.460 Å) and one longer distance with the S3 atom (2.914 Å). Once again, the Ag2-S distances are calculated with the Ag2 mode position. The average Ag2-S distance (2.590 Å) is in good agreement with that found for both the Ag(1) position in the crystal structure of stephanite (2.54 Å—Ribár and Nowacki 1970) and for the Ag position in the crystal structure of pyrrargirite,  $\text{Ag}_3[\text{SbS}_3]$  (2.573 Å—Engel and Nowacki 1966). In addition, it compares reasonably well with the value of 2.66 Å extrapolated from Shannon's tables (Shannon 1981). Finally,

**TABLE 2.** Fractional atomic coordinates, equivalent isotropic displacement parameters ( $\text{Å}^2$ ), and standard uncertainties (in parentheses) for samsonite

Atom	x	y	z	$U_{eq}$
<b>100 K</b>				
Mn	0	0	0.5	0.00674(19)
Sb	0.18530(2)	0.16043(3)	0.03909(4)	0.00684(6)
Ag1	0.31040(3)	0.23340(5)	0.57288(5)	0.01516(9)
Ag2	0.49642(4)	0.96855(5)	0.76015(6)	0.02510(11)
S1	0.09442(9)	0.26837(12)	0.34485(14)	0.0078(2)
S2	0.51780(9)	0.67229(12)	0.66814(14)	0.0078(2)
S3	0.26500(9)	0.41764(12)	-0.11521(14)	0.0080(2)
<b>300 K</b>				
Mn	0	0	0.5	0.01673(14)
Sb	0.184035(19)	0.16448(2)	0.03847(3)	0.01579(5)
Ag1	0.30710(7)	0.24815(11)	0.57129(10)	0.04309(12)
Ag2	0.49587(13)	0.97000(10)	0.76079(12)	0.06270(18)
S1	0.09171(8)	0.26901(9)	0.34369(11)	0.01627(15)
S2	0.51791(7)	0.67354(9)	0.66932(10)	0.01590(15)
S3	0.26400(7)	0.42128(10)	-0.11123(11)	0.01807(16)
<b>400 K</b>				
Mn	0	0	0.5	0.0220(3)
Sb	0.18327(3)	0.16638(5)	0.03790(5)	0.02142(10)
Ag1	0.30561(12)	0.2533(2)	0.57050(17)	0.0597(3)
Ag2	0.4960(2)	0.97038(19)	0.7609(2)	0.0822(3)
S1	0.09021(13)	0.26934(18)	0.34277(19)	0.0222(4)
S2	0.51847(12)	0.67407(17)	0.67019(18)	0.0214(3)
S3	0.26330(13)	0.42261(18)	-0.1099(2)	0.0241(4)

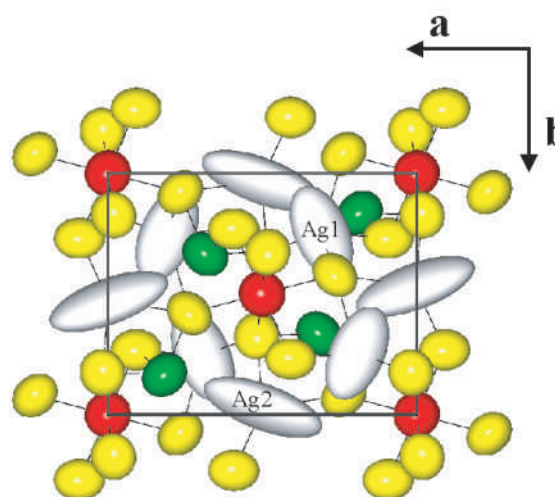


**FIGURE 3.** The crystal structure of samsonite down [001]. White, green, red, and yellow circles indicate Ag, Sb, Mn, and S, respectively. Ellipsoids are drawn at the 50% probability level. (Color is online only.)

**TABLE 3.** Anisotropic displacement parameters  $U_{ij}$  ( $\text{Å}^2$ ) and standard uncertainties for samsonite

Atom	$U_{11}$	$U_{22}$	$U_{33}$	$U_{12}$	$U_{13}$	$U_{23}$
<b>100 K</b>						
Mn	0.0066(3)	0.0071(3)	0.0064(3)	0.0002(3)	-0.0003(2)	0.0004(3)
Sb	0.00748(12)	0.00654(11)	0.00644(10)	0.00079(8)	-0.00021(7)	0.00031(8)
Ag1	0.01272(15)	0.02214(18)	0.01073(13)	-0.00658(11)	0.00194(10)	-0.00165(11)
Ag2	0.0464(3)	0.01153(16)	0.01732(16)	-0.01374(15)	0.00128(15)	-0.00302(12)
S1	0.0096(4)	0.0067(4)	0.0069(3)	-0.0001(3)	0.0001(3)	0.0002(3)
S2	0.0081(4)	0.0087(4)	0.0065(3)	0.0007(3)	-0.0004(3)	0.0006(3)
S3	0.0080(4)	0.0070(4)	0.0090(4)	-0.0015(3)	-0.0001(3)	0.0005(3)
<b>300 K</b>						
Mn	0.0168(3)	0.0178(3)	0.0157(2)	0.0005(2)	0.00148(18)	0.00025(19)
Sb	0.01591(8)	0.01611(8)	0.01541(8)	0.00237(6)	0.00141(5)	0.00059(6)
Ag1	0.03112(16)	0.0704(3)	0.02837(13)	-0.01957(16)	0.00785(12)	-0.00721(15)
Ag2	0.1105(4)	0.0302(2)	0.0476(2)	-0.0348(2)	0.0056(2)	-0.01010(16)
S1	0.0197(3)	0.0146(3)	0.0147(2)	0.0009(2)	0.0023(2)	0.0010(2)
S2	0.0154(3)	0.0184(3)	0.0139(2)	0.0008(2)	0.00080(19)	0.0018(2)
S3	0.0157(3)	0.0167(3)	0.0219(3)	-0.0029(2)	0.0008(2)	0.0019(2)
<b>400 K</b>						
Mn	0.0208(5)	0.0239(6)	0.0214(5)	0.0000(5)	0.0006(4)	0.0002(4)
Sb	0.02068(18)	0.02229(19)	0.02127(17)	0.00301(14)	0.00091(11)	0.00066(14)
Ag1	0.0425(3)	0.0982(6)	0.0392(3)	-0.0263(3)	0.0101(2)	-0.0106(3)
Ag2	0.1404(8)	0.0414(4)	0.0647(5)	-0.0455(5)	0.0051(4)	-0.0142(3)
S1	0.0264(7)	0.0211(7)	0.0192(6)	0.0012(5)	0.0026(5)	0.0021(5)
S2	0.0209(6)	0.0241(7)	0.0190(5)	0.0013(5)	0.0005(4)	0.0025(5)
S3	0.0209(6)	0.0225(7)	0.0288(6)	-0.0040(5)	-0.0004(5)	0.0019(5)

Mn exhibits an octahedral coordination with distances ranging from 2.607 to 2.628 Å.

The structural characteristics observed at 100 and 400 K are similar to those described for the room-temperature structure.

### DISCUSSION

The disordered character of a structure containing  $d^{10}$  ions can be easily evaluated by the analysis of the size and the shape of the anisotropic displacement parameters. The reason is that a strong anisotropy could reflect static or dynamic disorder related to positional disorder or anharmonicity of the fine structure. If we consider the room-temperature structure of samsonite projected down the  $c$  axis (Fig. 3), strongly anisotropic displacement parameters are observed for the silver cations, whereas the displacement ellipsoids for Mn, Sb, and S atoms are approximately isotropic. It is the aim of this paper to show that the strong anisotropy observed for the Ag cations is caused by static disorder

**TABLE 4.** Non-harmonic displacement parameters and standard uncertainty\* for samsonite

	Ag1	Ag2
<b>300 K</b>		
$C_{111}$	0.00007(9)	0.0010(4)
$C_{112}$	-0.00021(9)	0.0039(2)
$C_{113}$	0.00085(7)	0.0016(2)
$C_{122}$	-0.00222(16)	-0.00475(19)
$C_{123}$	0.00019(9)	0.00109(15)
$C_{133}$	0.00103(11)	-0.0030(3)
$C_{222}$	0.0163(5)	0.0040(2)
$C_{223}$	-0.0049(2)	-0.00124(16)
$C_{233}$	-0.00098(19)	0.0014(2)
$C_{333}$	0.0004(3)	-0.0021(5)
<b>400 K</b>		
$C_{111}$	0.0000(2)	0.0015(8)
$C_{112}$	-0.0002(2)	0.0064(5)
$C_{113}$	0.0017(2)	0.0018(5)
$C_{122}$	-0.0032(4)	-0.0079(5)
$C_{123}$	0.0001(2)	0.0016(4)
$C_{133}$	0.0018(3)	-0.0047(6)
$C_{222}$	0.0226(11)	0.0073(6)
$C_{223}$	-0.0073(6)	-0.0023(5)
$C_{233}$	-0.0042(5)	0.0023(6)
$C_{333}$	-0.0010(8)	-0.0045(14)

\* Third-order tensor elements  $C_{ijk}$  are multiplied by  $10^3$ .

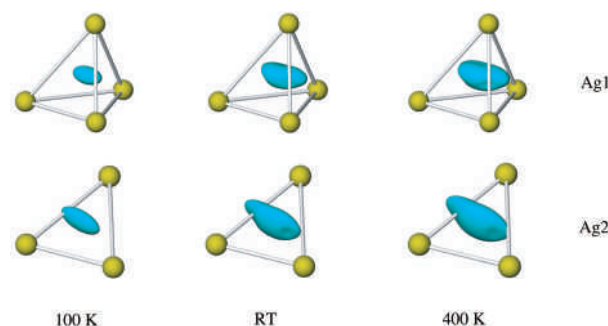


**FIGURE 4.** Non-harmonic probability density isosurfaces of Ag1 and Ag2 for samsonite at 100 K, RT, and 400 K. The size of the S atoms is arbitrary. Level of the 3D maps:  $0.03 \text{ \AA}^{-3}$ .

**TABLE 5.** Main distances and s.u. values (Å) for samsonite

	100 K	300 K	400 K
Mn-S3 (x2)	2.6060(9)	2.6073(8)	2.6095(13)
Mn-S1 (x2)	2.6074(9)	2.6161(7)	2.6213(14)
Mn-S2 (x2)	2.6188(9)	2.6283(7)	2.6318(13)
Sb-S1	2.4385(10)	2.4401(8)	2.4405(14)
Sb-S2	2.4633(9)	2.4605(7)	2.4603(13)
Sb-S3	2.4728(10)	2.4696(8)	2.4668(15)
Ag1*-S2	2.5652(10)	2.5649(7)	2.5704(13)
Ag1*-S3	2.6096(10)	2.6108(8)	2.5946(14)
Ag1*-S1	2.6593(10)	2.6633(7)	2.6555(13)
Ag1*-S3	2.6825(10)	2.7363(8)	2.7778(14)
Ag2*-S1	2.4077(10)	2.3968(7)	2.4085(14)
Ag2*-S2	2.4787(10)	2.4602(8)	2.4527(14)
Ag2*-S3	2.8637(10)	2.9139(7)	2.8939(13)

\* Distances calculated with refined positions at 100 K and mode positions at 300 and 400 K: Ag1 (0.3080,0.2438,0.5723) and Ag2 (0.5014,0.9660,0.7626) at 300 K, and Ag1 (0.3055,0.2507,0.5723) and Ag2 (0.5001,0.9647,0.7622) at 400 K.

and that it can be better modeled by means of a Gram-Charlier development of the anisotropic displacement factors.

In Figure 4 the  $pdf$  3D isosurfaces at 100 K, RT, and 400 K are reported for the Ag1 and Ag2 positions in the crystal structure of samsonite. As is typical for  $d^{10}$  elements, the probability density deformation increases the electron density toward the faces in the case of tetrahedral environment and toward the edges in the case of triangular environment. The deformation is very similar for both Ag1 and Ag2. Silver mode positions are calculated to be displaced by ca. 0.04 and 0.07 Å from the mean positions for Ag1 and Ag2, respectively. At 400 K, we have about the same situation as that at RT, although slightly more pronounced. At 100 K, however, there is no need for non-harmonic Gram-Charlier development of the Debye-Waller parameters. In addition, the equivalent atomic displacement parameters for all the atoms are much lower at low temperatures than at RT or 400 K. The fact that the Ag  $pdf$  changes shape as a function of temperature is a signature of a static disorder, and rules out anharmonic motion. However, no direct sign of ionic conductivity could be detected since no density was found between the Ag atoms, not even at the highest temperature. This observation does not preclude completely ionic conductivity, although it is most unlikely due to the rather large separation between the Ag atoms (ca. 3.24 Å).

Finally, let us consider the Ag behavior as a function of temperature. Gaudin et al. (1997) and van der Lee et al. (1993) studied the synthetic compounds  $\text{Ag}_2\text{Ti}_2\text{P}_2\text{S}_{11}$  and  $\text{Ag}_2\text{MnP}_2\text{S}_6$  by single-crystal X-ray diffraction and showed that the Ag atoms are observed to move from a lower coordination (triangular) to a higher coordination (tetrahedral) upon increasing the temperature. Surprisingly, in samsonite structure we observed the opposite situation with a smearing of the electron density toward the lower coordination sites with increasing the temperature.

### ACKNOWLEDGMENTS

The authors acknowledge CNR (Istituto di Geoscienze e Georisorse, sezione di Firenze) and M.I.U.R., P.R.I.N. 2005 project "Complexity in minerals: modulation, modularity, structural disorder" issued to Silvio Menchetti.

### REFERENCES CITED

Bachmann, R. and Schulz, H. (1984) Anharmonic potentials and pseudo potentials in ordered and disordered crystals. *Acta Crystallographica*, A40, 668–675.

- Becker, P.J. and Coppens, P. (1974) Extinction within the limit of validity of the Darwin transfer equations. I. General formalism for primary and secondary extinction and their applications to spherical crystals. *Acta Crystallographica*, A30, 129–147.
- Bindi, L., Evain, M., and Menchetti, S. (2006a) Temperature dependence of the silver distribution in the crystal structure of natural pearceite,  $(\text{Ag,Cu})_{16}(\text{As,Sb})_2\text{S}_{11}$ . *Acta Crystallographica*, B62, 212–219.
- (2006b) Complex twinning, polytypism and disorder phenomena in the crystal structures of antimonpearceite and arsenopolybasite. *Canadian Mineralogist*, in press.
- Bindi, L., Evain, M., Pradel, A., Albert, S., Ribes, M., and Menchetti, S. (2006c) Fast ionic conduction character and ionic phase-transitions in disordered crystals: The complex case of the minerals of the pearceite-polybasite group. *Physics and Chemistry of Minerals*, 33, 677–690.
- Boucher, F., Evain, M., and Brec, R. (1992) Single-crystal structure determination of  $\gamma\text{-Ag}_3\text{SiTe}_6$  and powder X-ray study of low-temperature  $\alpha$  and  $\beta$  phases. *Journal of Solid State Chemistry*, 100, 341–355.
- (1993) Distribution and ionic diffusion path of silver in  $\gamma\text{-Ag}_3\text{GeTe}_6$ : A temperature dependent anharmonic single crystal structure study. *Journal of Solid State Chemistry*, 107, 332–346.
- (1994) Second-order Jahn-Teller effect in  $\text{CdPS}_3$  and  $\text{ZnPS}_3$  demonstrated by a non-harmonic behaviour of  $\text{Cd}^{2+}$  and  $\text{Zn}^{2+}$   $d^{10}$  ions. *Journal of Alloys and Compounds*, 215, 63–70.
- Brandenburg, K. (2001) Diamond version 3. Crystal Impact GbR, Bonn, Germany.
- Edenharter, A. and Nowacki, W. (1974) Verfeinerung der Kristallstruktur von Samsonit,  $(\text{SbS}_3)_2\text{Ag}_2^{\text{III}}\text{Ag}_2^{\text{IV}}\text{Mn}^{\text{VI}}$ . *Zeitschrift für Kristallographie*, 140, 87–99.
- Engel, P. and Nowacki, W. (1966) Die Verfeinerung der Kristallstruktur von Proustit,  $\text{Ag}_3\text{AsS}_3$ , und Pyrargyrit,  $\text{Ag}_3\text{SbS}_3$ . *Neues Jahrbuch für Mineralogie Monatshefte*, 181–195.
- Evain, M., Gaudin, E., Boucher, F., Petricek, V., and Taulelle, F. (1998) Structures and phase transitions of the  $\text{A}_7\text{PSe}_6$  ( $\text{A} = \text{Ag, Cu}$ ) argyrodite-type ionic conductors. I.  $\text{Ag}_7\text{PSe}_6$ . *Acta Crystallographica*, B54, 376–383.
- Evain, M., Bindi, L., and Menchetti, S. (2006a) Structure and phase transition in the Se-rich variety of antimonpearceite,  $(\text{Ag}_{14.67}\text{Cu}_{1.26}\text{Bi}_{0.01}\text{Pb}_{0.01}\text{Zn}_{0.01}\text{Fe}_{0.03})_{15.93}(\text{Sb}_{1.86}\text{As}_{0.19})_{2.05}(\text{S}_{8.47}\text{Se}_{2.55})_{11.02}$ . *Acta Crystallographica*, B62, 768–774.
- (2006b) Structural complexity in minerals: twinning, polytypism and disorder in the crystal structure of polybasite,  $(\text{Ag,Cu})_{16}(\text{Sb,As})_2\text{S}_{11}$ . *Acta Crystallographica*, B62, 447–456.
- Gaudin, E., Fischer, L., Boucher, F., Evain, M., and Petricek, V. (1997)  $\text{Ag}_2\text{Ti}_2\text{P}_2\text{S}_{11}$ : A new layered thiophosphate. Synthesis, structure determination and temperature dependence of the silver distribution. *Acta Crystallographica*, B53, 67–75.
- Gaudin, E., Boucher, F., and Evain, M. (2001) Some factors governing  $\text{Ag}^+$  and  $\text{Cu}^+$  low coordination in chalcogenide environments. *Journal of Solid State Chemistry*, 160, 212–221.
- Herrendorf, W. (1993) Habitus. Ph.D. dissertation, University of Karlsruhe, Germany.
- Johnson, C.K. and Levy, H.A. (1974) Thermal-motion analysis using Bragg diffraction data. In J.A. Ibers and W.C. Hamilton, Eds., *International Tables for X-ray Crystallography*, IV, p. 311–336. Kynoch Press, Birmingham.
- Kuhs, W.F. (1992) Generalized atomic displacements in crystallographic structure analysis. *Acta Crystallographica*, A48, 80–98.
- Kuhs, W.F. and Heger, G. (1979) Neutron diffraction study of copper sulfide bromide  $(\text{Cu}_6\text{PS}_3\text{Br})$  at 293 K and 473 K. In P. Vashishta, J.N. Mundy, and G.K. Shenoy, Eds., *Fast ion transport in solids: Electrodes and Electrolytes*, p. 233–236. Elsevier, Amsterdam.
- Pertlik, F. (1994) Hydrothermal synthesis and crystal structure determination of heptasilver(I)-disulfur-tetrathioarsenate(V),  $\text{Ag}_7\text{S}_2(\text{AsS}_4)$ , with a survey on thioarsenate anions. *Journal of Solid State Chemistry*, 112, 170–175.
- Petricek, V. and Dusek, M. (2000) JANA2000, a crystallographic computing system. Institute of Physics, Academy of Sciences of the Czech Republic, Prague, Czech Republic.
- Petricek, V., Dusek, M., and Palatinus, L. (2006) JANA2006 (beta version), a crystallographic computing system. Institute of Physics, Academy of Sciences of the Czech Republic, Prague, Czech Republic.
- Ribár, B. and Nowacki, W. (1970) Die Kristallstruktur von Stephanit,  $[\text{SbS}_3]_3[\text{S}/\text{Ag}_5^{\text{III}}]$ . *Acta Crystallographica*, B26, 201–207.
- Shannon, R.D. (1981) Bond distances in sulfides and a preliminary table of sulfide crystal radii. In M. O’Keeffe and A. Navrotsky, Eds., *Structure and bonding in crystals*, II, p. 53–70. Academic Press, New York.
- Stoe and Cie (1996) X-shape (ver. 1.02). Stoe and Cie, Darmstadt, Germany.
- Trueblood, K.N., Bürgi, H.-B., Burzlaff, H., Dunitz, J.D., Gramaccioni, C.M., Schulz, H., Shmueli, U., and Abrahams, S.C. (1996) Atomic displacement parameter nomenclature. Report of a subcommittee on atomic displacement parameter nomenclature. *Acta Crystallographica*, A52, 770–781.
- van der Lee, A., Boucher, F., Evain, M., and Brec, R. (1993) Temperature dependence of the silver distribution in  $\text{Ag}_2\text{MnP}_2\text{S}_6$  by Single Crystal X-ray Diffraction. *Zeitschrift für Kristallographie*, 203, 247–264.
- Zucker, U.H. and Schulz, H.H. (1982) Statistical approaches for the treatment of anharmonic motion in crystals. II. Anharmonic thermal vibrations and effective atomic potentials in the fast ionic conductor lithium nitride ( $\text{Li}_3\text{N}$ ). *Acta Crystallographica*, A38, 568–576.

MANUSCRIPT RECEIVED JUNE 23, 2006

MANUSCRIPT ACCEPTED DECEMBER 22, 2006

MANUSCRIPT HANDLED BY SERGEY KRIVOVICHEV